Macromolecules

pubs.acs.org/Macromolecules Article

Further Proof of Unconventional Conjugation via Disiloxane Bonds: Double Decker Sesquioxane [vinylMeSi$(O_{0.5})_2$(PhSi$O_{1.5})_8$$(O_{0.5})_2$SiMevinyl] Derived Alternating Terpolymers Give Excited-State Conjugation Averaging That of the Corresponding Copolymers

Zijing Zhang, Jun Guan, Ramin Ansari, John Kieffer, Nuttapon Yodsin, Siriporn Jungsuttiwong, and Richard M. Laine*

Cite This: *Macromolecules* 2022, 55, 8106–8116 Read Online

ACCESS | Metrics & More | Article Recommendations | Supporting Information

ABSTRACT: Here, we report the synthesis of DD SQ terpolymers with alternating biphenyl/terphenyl/stilbene and thiophene/hexylthiophene/bithiophene/thienothiophene linkers. These terpolymers were characterized using ^{1}H and ^{13}C nuclear magnetic resonance, gel permeation chromatography, matrix-assisted laser desorption/time-of-flight spectrometry, thermogravimetric analysis, and Fourier-transform infrared with the goal of combining long-wavelength emissions with high quantum yields. Density functional theory modeling studies using the Vienna ab initio simulation package and Gaussian 16 methods were also explored in attempts to determine HOMO-LUMO electronic configurations. Terpolymers' UV−vis properties demonstrate an emission intermediate between the respective copolymers rather than emission from both units as would be expected from physical mixtures, supporting electronic communication along polymer chains and through cages linked via disiloxane units as seen in previous reports on copolymers of the same systems. In addition, terpolymers of DD, thiophene, and terphenyl/stilbene offer Φ_F that improved from 0.09 for DD/thiophene to 0.20 and 0.24, respectively. Compared to the corresponding terphenyl and stilbene copolymers, terpolymers display 35 nm red-shifted emissions, suggesting that it is possible to combine features of both copolymers in a single terpolymer, suggesting new opportunities to tailor photophysical properties by modifying structures, especially in systems with disiloxane linkers.

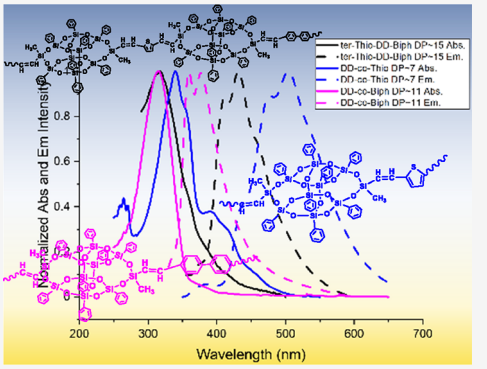

INTRODUCTION

Silsesquioxanes (SQs) have received considerable recent attention in part due to their well-defined nanostructures with high degrees of symmetry and in part because of their high rigidity and ability to be functionalized using multiple different and complementary approaches. They also offer very high thermal and often mechanical stability engendered by their silica cage nanostructures, as evidenced by the multiple reviews and one book published on these compounds and materials made therefrom.[1−17]

In addition to their outstanding and highly manipulable physical properties, they also offer unique and unexpected photophysical properties belying what was originally thought to be simply organic decorated silica. To this end, our group and others have reported that aromatic and vinyl functionalized SQs ($T_{8,10,12}$) exhibit LUMOs that reside in the cage centers.[18,19] As a consequence, functionalizing such cages with organic chromophores results in extended conjugation reflecting interactions between these chromophores and the cage LUMOs, leading to extensive red-shifts in emissions.[20]

Still more recently, in an effort to identify the limits wherein SQ structures exhibit LUMOs capable of conjugating with appended conjugated moieties, we extended our efforts to both corner missing (T_7) and doubly open cage structures, finding that even these structures offer LUMOs that couple with conjugated moieties.[21] Indeed, in the corner missing cages, emission Φ_F values are significantly enhanced vs simple stilbenes increasing from 0.05 to 0.10 to >0.70. This suggests that the excited state LUMO is cage-centered and protected from radiationless decay.

Received: July 1, 2022
Revised: August 18, 2022
Published: September 13, 2022

https://doi.org/10.1021/acs.macromol.2c01355
Macromolecules 2022, 55, 8106−8116

The next effort along these lines was to replace T_8 SQs with both phenyl-substituted double decker (DD) and ladder (LL) SQs wherein functionalization on the DD phenyls also resulted in the formation of cage-centered LUMOs.[22,23] In these systems, we were also able to copolymerize vinyl-capped DD and LL systems with a large number of aromatic monomer units including phenyl, biphenyl, terphenyl, thiophene, thienothiophene, and bithiophene. At the outset, we assumed that, because each DD and LL segment of the copolymers contains two −O−Si(Me,vinyl)−O end caps, there would be no opportunity for conjugation. This was especially likely for the LL SQs since they also lack a cage structure.

Much to our surprise, the LL SQ copolymers show even further red-shifted emissions compared to the DD systems, suggesting superior conjugation and greatly changing our perspective of how conjugation manifests in these systems. Indeed, to date, we are still unsure of the actual mechanisms of conjugation. These results provided the motivation to further probe conjugation via −O−Si(Me,vinyl)−O units in terpolymers where one would expect averaging of the emission between the two co-monomeric units.

It is important to note that easily processed polymers with red, green, and blue emissions with high absorption and emission quantum efficiencies (Φ_F = photons out/photons in) are highly desirable in multiple flat panel display applications, especially if they offer robust properties vis a vis thermal and oxidative stabilities.

Given that the Φ_F of the phenyl, biphenyl, and terphenyl DD copolymers are >70% but with emissions mostly near 390 nm, whereas the thiophene copolymers emit much further red but with Φ_F < 20%, we also were interested in exploring the idea that coupling the two types of comonomers might increase Φ_F while also shifting emission wavelengths further into the visible as possible routes to robust PLED type materials.

EXPERIMENTAL SECTION

Materials. All purchased chemicals were used as received unless otherwise indicated. Tetrasilanol phenylsilsesquioxane $[PhSiO_{1.5}]_8[O_{0.5}H]_4$ $[DD(OH)_4)]$ was purchased from Hybrid Plastics. Vinylmethyldichlorosilane $vinylMeSiCl_2$, tris(dibenzylideneacetone)dipalladium(0) $Pd_2(dba)_3$, bis(tri-*tert*-butylphosphine)palladium(0) $Pd[P(t\text{-}Bu)_3]_2$, *N*,*N*-dicyclohexylmethylamine NCy_2Me, *N*-acetyl-L-cysteine, 4,4′-dibromo-1,1′-biphenyl, 4,4″-dibromo-*p*-terphenyl, 4,4′-dibromo-*trans*-stilbene, 2,5-dibromothiophene, 2,5-dibromo-3-hexylthiophene, 5,5′-dibromo-2,2′-bithiophene, and 2,5-dibromothieno[3,2-*b*]thiophene were purchased from Sigma-Aldrich. Triethylamine (Et_3N) and THF were distilled under nitrogen from sodium/benzophenone ketyl.

Syntheses. VinylDDvinyl was synthesized as described previously.[24]

General Heck Cross-Coupling of VinylDDvinyl with Br-Ar1-Br (Ar1 = Thiophene, Hexylthiophene, Bithiophene, and Thienothiophene).[22] To a dry 200 mL Schlenk flask under N_2 were added 3.62 g (3.0 mmol) of vinylDDvinyl and 38.7 mg (0.08 mmol) of $Pd[P(t\text{-}Bu)_3]_2$ followed by 45 mL of distilled THF, 0.80 g (4.0 mmol) of NCy_2Me, and Br-Ar1-Br (1.0 mmol). The mixture was stirred magnetically at 70 °C and tracked by GPC. The reaction was quenched after 2 days by filtering through 1 cm Celite, which was washed with THF (5 mL). The resulting filtrate was concentrated by rotary evaporation, the resulting concentrated solution was then precipitated into 150 mL of cold, well-stirred methanol and filtered, and the colored solid was redissolved in 10 mL of THF. The solution was then filtered again through a 1 cm Celite column to further remove residual Pd particles, concentrated, and reprecipitated into 100 mL of cold, stirred methanol to give an ∼85% yield of the crude colored product for most reactions studied. The two-cage product (vinylDD-Ar1-DDvinyl) was then isolated using column chromatography (DCM:hexane 1:2 volume ratio, silica gel).

General Heck Polymerization of VinylDD-Ar1-DDvinyl with Br-Ar2-Br (Ar2 = Biphenyl, Terphenyl, and Stilbene). To a dry 50 mL Schlenk flask under N_2 were added above vinylDD-Ar1-DDvinyl (0.04 mmol) and 4.0 mg (0.008 mmol) of $Pd[P(t\text{-}Bu)_3]_2$ followed by 20 mL of distilled THF, 64 mg (0.32 mmol) of NCy_2Me, and Br-Ar2-Br (0.04 mmol). The mixture was stirred magnetically at 70 °C and tracked by GPC. The reaction was quenched after 14 days by filtering through 1 cm Celite, which was washed with THF (5 mL). The resulting filtrate was concentrated by rotary evaporation, and the resulting concentrated solution was then precipitated into 100 mL of cold, well-stirred methanol to give a yield of 75% colored product.

Mixing F_4TCNQ with Alternating Terpolymers. To a 2 mL vial, 5 mg of a solid alternating terpolymer in 0.3 mL of DCM was added and then different volumes of F_4TCNQ/DCM (2 mg/mL) solutions were added slowly on the top of the terpolymer solution. Other terpolymer solutions with different molar ratios of F_4TCNQ dopant were prepared using the same procedure. FTIR and UV−vis spectrometry of the alternating terpolymers mixed with F_4TCNQ were measured.

Analytical Methods. Matrix-assisted laser desorption/time-of-flight spectrometry (MALDI-TOF), ^1H and ^{13}C nuclear magnetic resonance (NMR), thermogravimetric analyses (TGA), gel permeation chromatography (GPC), and Fourier-transform infrared spectroscopy (FTIR) measurements were done as described in ref 21.

Photophysical Characterization. *UV−Vis Spectrometry.* UV−vis measurements were recorded on a Shimadzu UV-1601 UV−vis transmission spectrometer. Samples were dissolved in DCM and diluted to a concentration (10^{-3} to 10^{-4} M) where the absorption maximum was <10% for a 1 cm path length.

Photoluminescence Spectrometry. Photoluminescence spectra were recorded on a Fluoromax-2 fluorometer in the required solvent using 300 nm excitation. Samples from UV−vis spectroscopy were diluted (10^{-5} to 10^{-6} M) to avoid excimer formation and fluorometer detector saturation.

Photoluminescent Quantum Yields. Quantum yields were measured using an integrated sphere. Samples were dissolved in CH_2Cl_2 (DCM) and diluted to a concentration (10^{-3} to 10^{-4} M) where the absorption maximum was <10% for a 1 cm path length. Absorption and emission inside the sphere were determined by comparison to a blank CH_2Cl_2 in cuvette (glass only). Each sample was measured three times or more.

Molar Extinction Coefficients (ε). Molar extinction coefficients (ε) were calculated as $\varepsilon = A/cl$, where A = absorbance, c = sample concentration in moles/liter, and l = length of the light path through the sample in centimeters. All the samples were dissolved in DCM. The cuvettes used for the absorption test have an inner dimension of 1.0 cm.

Modeling Methods.

(1) Ground state optimized structures of all structures were determined using DFT at the B3LYP/6-31G(d,p) level of theory with GD3BJ dispersion correction.[25−28] The vertical excitation energies and electronic absorption spectra were investigated using time-dependent density functional theory (TD-DFT) with hybrid exchange-correlation functional CAM-B3LYP. All calculations were run with the Gaussian 16 program package.

(2) Crystal state calculations were performed using plane-wave DFT within the framework of non-spin-polarized density functional theory using the Vienna ab initio simulation package (VASP). The exchange-correlation energy and potential were described by Perdew, Burke, and Ernzerhof (PBE) potentials.[29,30] The electron−ion interactions were described by the projector-augmented wave (PAW) scheme. The many body dispersion method of Tkatchenko et al.[31] was used to account for van der Waals interactions. Van der Waals interactions have a huge impact on the electronic properties of double-decker copolymers since the molecules and different functional groups in the same molecule are very close to one another.

https://doi.org/10.1021/acs.macromol.2c01355
Macromolecules 2022, 55, 8106−8116

Scheme 1. Syntheses of DD Derived Alternating Terpolymers

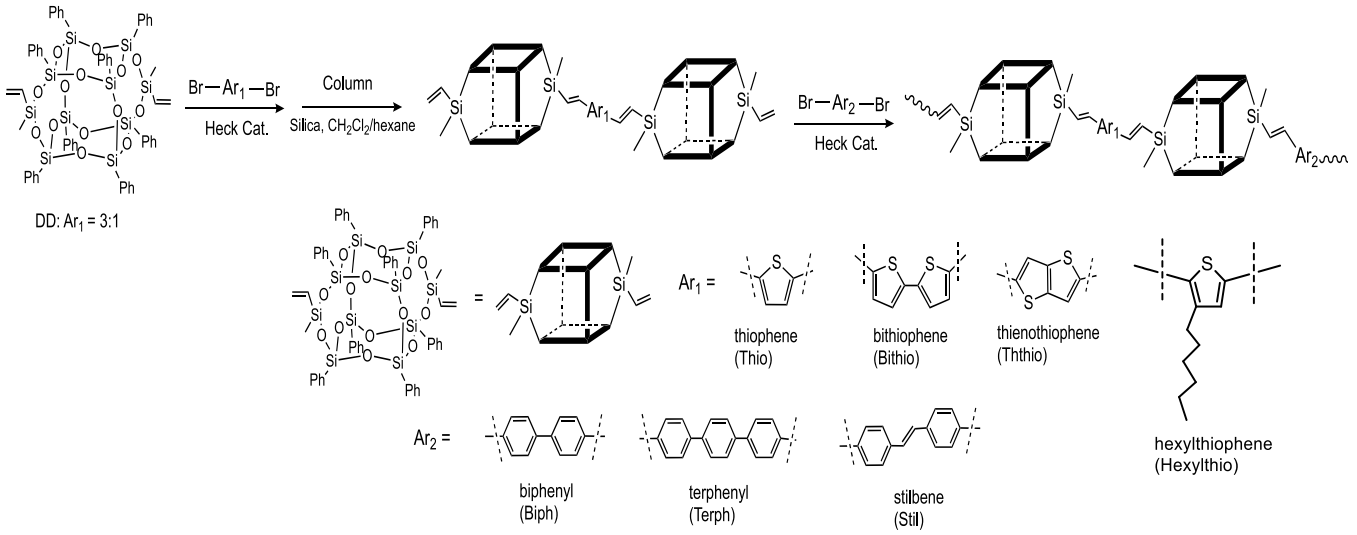

Table 1. MALDI-TOF, GPC, and TGA Data for Terpolymers

		GPC			TGA		
compound	MALDI-TOF m/z[a]	M_n	M_w	$Đ$	ceramic yield %	theory yield %	$T_{d5\%/air}$ °C
DD-thio-DD	2600[c]	1690	1770	1.05	48	48	545
ter-thio-DD-biph	2745[c]	4676	13,215	2.83	44	45	500
ter-thio-DD-terph	2822[c]	4500	7400	1.65	45	44	520
ter-thio-DD-stil	2764[c]	17,213	57,111	2.97	44	45	410
DD-hexylthio-DD	2679[c]	1434	1468	1.02	45	47	450
ter-hexylthio-DD-biph	2831[c]	9397	20,837	2.22	42	44	480
ter-hexylthio-DD-terph	2906[c]	6333	13,934	2.20	40	43	460
ter-hexylthio-DD-stilbene	2854[c]	5125	14,420	2.81	39	44	300
DD-bithio-DD	2574[b], 2682[a]	1780	1890	1.06	45	47	540
ter-bithio-DD-biph	2827[c]	3113	5112	1.64	44	44	410
ter-bithio-DD-terph	2905[c]	10,053	25,622	2.55	43	43	350
ter-bithio-DD-stil	2855[c]	21,208	55,885	2.63	37	44	320
DD-thithio-DD	2655[c]	1720	1790	1.04	46	47	530
ter-thithio-DD-biph	2803[c]	4935	7996	1.62	44	44	400
ter-thithio-DD-stilbene	2827[c]	4701	23,164	4.93	41	44	370

[a]As Ag^+ adduct. [b]As H^+ adduct. [c]m/z of the repeating unit of terpolymers.

RESULTS AND DISCUSSION

Our objectives continue to be to map structure−property relationships of hybrid polymers with SQs in the main chain. We are particularly interested in exploring the possible effects of introducing different conjugated linkers on emissive behavior with the idea of modifying and tailoring their photophysical properties such that they may offer novel materials for display applications. We are also particularly interested in expanding our knowledge of the factors leading to unconventional conjugation in the excited state, especially via disiloxane linkages, contrasting with traditional views of such insulating linkers.

Syntheses. Occam's razor suggests that the simplest approach should be tried first. Thus, the direct copolymerization with a 2:1:1 molar ratio of vinylDDvinyl:dibromo-biphenyl:dibromo-thiophene was explored. However, divinylDD reacts with biphenyl much faster than with thiophene such that that no terpolymer forms. Instead, it appears that block copolymers form with larger segments of DD-*co*-biphenyl. It is likely that the thiophene sulfur binds reversibly to Pd such that catalytic efficiency is decreased.[32−35] This is also the simplest explanation for why both DD/LL SQ derived copolymers with phenyl systems always generate much longer chains (degree of polymerization, DP ∼15) than thiophene systems (DP ∼5).

Thus, we turned to the more tedious approach to alternating terpolymers using step-by-step syntheses per Scheme 1. We first coupled thiophene groups with DD SQs on both ends via Heck cross-coupling and with a 3:1 DD:thiophene molar ratio. The expected vinylDD-thiophene-DDvinyl was isolated via column chromatography (DCM:hexane 2:1 volume ratio). The reason for choosing thiophene systems in the first step is again that the polymerization of vinylDD-biphenyl-DDvinyl with thiophene will be even more difficult in any efforts to obtain longer terpolymers. Thus, vinylDD-thiophene-DDvinyl was synthesized first. All the products were characterized using standard methods, as recorded in Table 1 and Figures S1 and S2.

Figure 1a and Table 1 record GPC data for these compounds. After Heck catalytic cross-coupling of divinyl-DD with a 3:1 molar ratio dibromo-Ar1, the product is a mixture of single-cage, two-cage, and three-cage products as

https://doi.org/10.1021/acs.macromol.2c01355
Macromolecules 2022, 55, 8106−8116

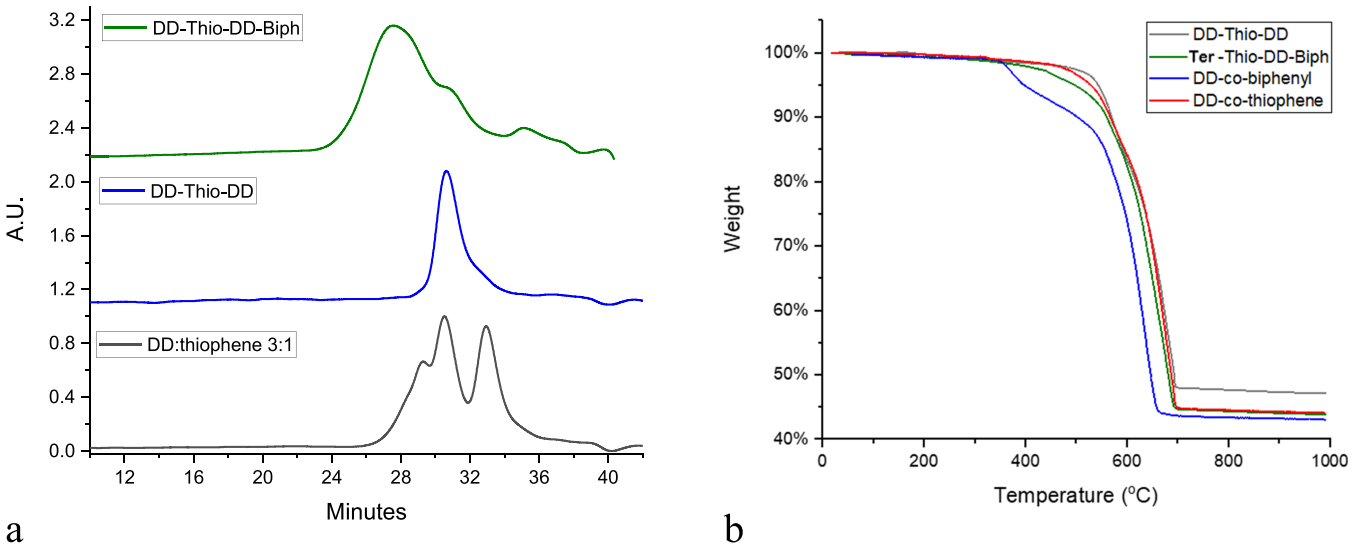

Figure 1. (a) GPC of the product mixture of DD with thiophene (3:1 molar ratio), isolated DD-thiophene-DD via column chromatography, and terpolymer of DD-thiophene-DD with biphenyl. (b) TGA of DD-thiophene-DD, ter-thio-DD-biph, and copolymers of DD-*co*-biphenyl and DD-*co*-thiophene.

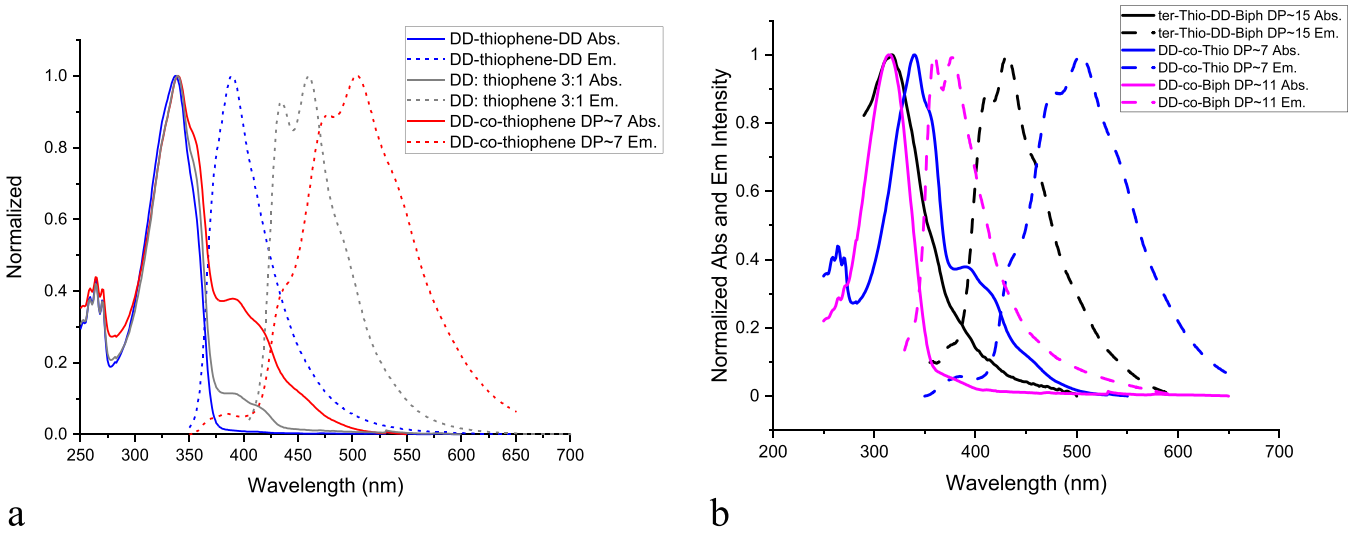

Figure 2. (a) Normalized absorption and emission of DD-thiophene-DD, mixture of DD:thiophene 3:1, and longer DD-*co*-thiophene (1:1). (b) Absorption and emission of ter-thio-DD-biph and corresponding copolymers, DD-*co*-biphenyl and DD-*co*-thiophene.

expected and evidenced by three narrow peaks (PDI ∼1.04) at retention times of 32.9, 30.5, and 29.3 min, respectively, due to the differences in hydrodynamic volumes of the intact SQ cores. The target product, DD-Ar1-DD, is the second peak in the GPC trace and can be isolated via column chromatography.

Figures S1−S4 provide MALDI data for the dimers. The TGA in Figure 1b and data in Table 1 were used to characterize the end groups of the isolated two-cage product, which indicate end-capping of Ar1 with DD cages according to the expected m/z in MALDI and ceramic yields close to or the same as the theoretical values calculated from the chemical formulae for DD-Ar1-DD. Note that the molecular weights suggested by GPC are always smaller than MALDI due to the sphere-like hydrodynamic volume of the DD cores.

The successful isolation of DD-Ar1-DD is also supported by ^{1}H and ^{13}C NMRs in Figures S30, S33, S34, S43, and S44 and Table S1. The ^{1}H NMR of DD-thiophene-DD exhibits new signals for ethene groups bonded to thiophene at 6.9 and 6.4 ppm, distinct from peaks for unreacted vinyl groups at 6.20 and 6.05 ppm. The theoretical ratio of reacted to unreacted vinyl protons is 2:3, matching the actual integration ratio of 2.1:3.1. Additionally, there are two methyl peaks, likely indicating protons in two magnetically different environments originating from reacted and unreacted vinyls. The ^{13}C NMR shows peaks for phenyl groups on the DD cage from 127 to 134 ppm. Reacted and unreacted vinyl groups also display distinct chemical shifts at 144.3 and 139.1 ppm and 135.2 and 134.5 ppm, respectively. Thiophene carbon peaks appear at ≈137 and 124 ppm.

Peaks are assigned by comparison with the NMR of di-vinyl DD. The isolated dimer products are also characterized by FTIR, as shown in Figures S45−S48 and peak assignments in Table S2, with the highest peak at 1132 cm^{-1} from the Si−O−Si framework. Peaks from νC═C and νC−H are also observed

https://doi.org/10.1021/acs.macromol.2c01355
Macromolecules 2022, 55, 8106−8116

Table 2. UV−Vis, Photoluminescent Data, Quantum Efficiency (Φ_F), and Molar Extinction Coefficient (ε) for DD Derived Copolymers and Terpolymers

polymers	DP	Abs. λ_{max} (nm)[a]	Em. λ_{max} (nm)[a]	Φ_F	$\varepsilon \times 10^4$
DD-*co*-thiophene	7	340	478, 505	0.09 ± 0.001	1.0
DD-*co*-bithiophene	4	391	505, 538	0.17 ± 0.02	0.7
DD-*co*-thienothiophene	5	358	496, 526	0.13 ± 0.01	0.9
DD-*co*-hexylthiophene		277, 345	478		
DD-*co*-biphenyl	11	314	357, 373	0.66 ± 0.05	0.5
DD-*co*-terphenyl	11	321	374, 392	0.87 ± 0.04	0.6
DD-*co*-stilbene	9	357	393, 412, 436	0.61 ± 0.04	0.4
DD-thio-DD	2	340	390	0.03 ± 0.003	2.2 ± 0.08
DD-hexylthio-DD	2	345	440	0.10 ± 0.02	1.7 ± 0.11
DD-bithio-DD	2	387	436, 461	0.13 ± 0.006	3.3 ± 0.06
DD-thithio-DD	2	358	400, 412	0.08 ± 0.03	3.7 ± 0.04
ter-thio-DD-biph	15	317	409, 432	0.07 ± 0.004	5.7 ± 0.02
ter-thio-DD-terph	8	324	415, 427	0.20 ± 0.03	6.8 ± 0.12
ter-thio-DD-stil	64	343, 355	415, 446, 469	0.24 ± 0.06	3.7 ± 0.03
ter-hexylthiophene-DD-biphenyl	28	311	430	0.25 ± 0.028	4.9 ± 0.11
ter-hexylthiophene-DD-terphenyl	19	321	412	0.16 ± 0.036	3.0 ± 0.11
ter-hexylthiophene-DD-stilbene	20	344	392, 412, 438	0.25 ± 0.033	9.4 ± 0.16
ter-bithio-DD-biph	5	312, 378	437, 464, 495	0.14 ± 0.004	5.6 ± 0.23
ter-bithio-DD-terph	27	322, 390	437, 464, 495	0.12 ± 0.01	7.7 ± 0.83
ter-bithio-DD-stil	59	357	460	0.15 ± 0.01	5.3 ± 0.12
ter-thithio-DD-biph	9	316	411, 433, 451	0.14 ± 0.02	5.4 ± 0.22
ter-thithio-DD-stil	26	357	467	0.25 ± 0.036	7.5 ± 0.57

[a]Underlined peaks are considered the primary absorption and emission λ_{max}.

around 1400 and 3000 cm^{-1}, respectively, characteristic of phenyl, vinyl, and thiophene groups.

After Heck cross-coupling of DD-Ar1-DD with dibromo-Ar2, the alternating terpolymers DD-Ar1-Ar2 appear in the GPC with retention times of 25−28 min, with a $Đ$ of ∼1.7 expected for step-growth type polymerization with average DPs of 4−8. The presence of oligomers is also confirmed by MALDI, which shows peaks every DD-Ar1-DD-Ar2 repeat unit.

In general, SQ monomers are readily ionizable; however, as the M_w of SQ-based oligomers increases, the ionization efficiency decreases, resulting in smaller peaks. Thus, MALDI peak heights cannot be considered as a quantitative measure of the amount of each species in the oligomeric mixture. From the TGA analyses, the $T_{d5\%}$ of the resulting terpolymers are all >400 °C, indicating that high thermal stabilities in air and the ceramic yields are close to the theoretical value and in between those of the corresponding copolymers DD-co Ar1/Ar2. ^1H NMR in Table S1 and Figure S30 suggests only trace amounts of end vinyl groups around 6.10 ppm and greater amounts of ethene bridges between the DD cage and organic tethers Ar1 and Ar2 around 7.0 and 6.5 ppm, respectively, indicating successful polymerization. Finally, there are broad peaks in the aromatic proton region around 7.8−7.1 ppm, typical for these compounds and peaks in the CH_3 region around 0.45 ppm. There are essentially no significant changes in FTIRs as expected.

Photophysical Properties. We previously reported the successful preparation of a series of DD copolymers/oligomers and the discovery of through-chain conjugation in the excited state even through the −O−Si(Me,vinyl)−O siloxane units as evidenced by the exceptional red-shifted emission from the respective model compounds.[22,23] Figure 2a compares the UV−vis absorption and emission of DD-thiophene-DD, short oligomers, and long DD-*co*-thiophene synthesized using the ratios of DD:thiophene of 3:1 and 1:1, respectively.

It is worth noting that the emission maxima show progressive red-shifts from 390 to 465 to 505 nm as a function of chain length. In addition, even though the Abs. λ_{max} at 340 nm does not change, the absorption shoulder around 400 nm grows with extensions in chain length further supporting the presence of through-chain conjugation involving the SQ cages via siloxane units. DD-bithiophene-DD and DD-thienothiophene-DD spectra are presented in Figures S54 and S55 and also show similar progressively red-shifted emissions with increasing chain lengths.

Figure 2b provides absorption and emission data for the ter-thio-DD-biph and the corresponding DD-*co*-biphenyl and DD-*co*-thiophene, as summarized in Table 2. The absorption spectrum of the alternating terpolymer shows a peak at 315 nm around the Abs. λ_{max} of DD-*co*-biphenyl and an increased shoulder around 400 nm, similar to DD-*co*-thiophene, which suggests successful Heck polymerization and no ground-state HOMO interactions. The Em. λ_{max} of the terpolymer is 430 nm, in between that of DD-*co*-biphenyl (375 nm) and DD-*co*-thiophene (505 nm), which again points to the excited-state conjugation involving SQ cages and two different conjugated linkers and the opportunities to tune the emission of DD derived polymers. Compared to the starting DD-thiophene-DD, the Em. λ_{max} of terpolymer is red-shifted by 40 nm, indicating extended conjugation after linking biphenyl with DD-thiophene-DD.

On excitation near the Abs. λ_{max} of DD-*co*-biphenyl (315 nm) and DD-*co*-thiophene (340 nm), the Em. λ_{max} remains at 430 nm while the intensity is much higher for excitation at 345 nm, as shown in Figure S61. As indicated in Table 2 and Figures S62−S71, other terpolymers also show emission maxima between those of the two copolymers, all suggesting

https://doi.org/10.1021/acs.macromol.2c01355
Macromolecules 2022, 55, 8106−8116

that the polymer LUMOs communicate between SQs through each type of conjugated unit.

Photoluminescence quantum yields were measured using a K-sphere integrating sphere in DCM with the excitation wavelengths at Abs. λ_{max} of DD-*co*-Ar1 to explore the effect of incorporation of Ar2 into the system since DD-*co*-Ar2 displays a quite high Φ_F. Table 2 shows that the incorporation of biphenyl offers minimal improvement in Φ_F since the terpolymers display essentially the same Φ_F as those of the corresponding copolymers.

Terpolymers of ter-thio-DD-terph and ter-thio-DD-stil exhibit improved Φ_F from 0.09 to 0.20 and 0.24, respectively. Both ter-thio-DD-biph and ter-thio-DD-stil show red-shifted emissions by ∼35 nm from corresponding DD-*co*-biphenyl and DD-*co*-stilbene. These two systems are successful examples combining longer-wavelength emission and higher quantum yields. Unfortunately, the bithiophene and thienothiophene derived terpolymers offer no significant increases in observed quantum yields, which are similar to those of DD-*co*-bithiophene and DD-*co*-thienothiophene of ∼0.15. More studies need to be done to explore suitable combinations of organic tethers targeting novel (superior) photophysical properties important for display devices.

Finally, we recently prepared LL copolymers analogous to the DD copolymers, and among them, LL-*co*-biphenyl, terphenyl, and stilbene offer quantum yields of 0.6 but further red-shifted emission beyond their DD analogues. Studies of LL derived terpolymers may offer superior photophysical properties while still maintaining robust thermal behavior.

As a further proof of through cage conjugation and along polymer chains, we also assessed the electron donating properties of these terpolymers using 2,3,5,6-tetrafluoro-7,7,8,8-tetracyanoquinodimethane (F_4TCNQ) as done in our recent paper.[22] As previously, we also see charge transfer that can be detected by FTIR most easily by shifts in the cyano stretching vibrations.

The charge transfer studies between F_4TCNQ and the double decker alternating terpolymers in Table 3 provide further evidence of unconventional conjugation. Compounds ter-hexyl-thiophene-DD-biphenyl, ter-hexylthiophene-DD-terphenyl, ter-hexylthiophene-DD-stilbene, ter-thiophene-DD-stilbene, ter-bithiophene-DD-stilbene, and ter-thienothiophene-DD-stilbene exhibit almost integer charge transfer (ICT) with 50 mol % electron acceptor F_4TCNQ. The partial charge degrees calculated are more than 0.9. The inherent error may simply be due to the width of the peak. Among them, ter-hexylthiophene-DD-biphenyl, ter-hexylthiophene-DD-terphenyl, ter-thiophene-DD-stilbene, and ter-thienothiophene-DD-stilbene show both integer charge transfer and partial charge transfer on changing content using excess F_4TCNQ, consistent with evidence of an absorption peak at 390 nm, indicative of excess neutral F_4TCNQ. Color changes from light greenish yellow to grass green could be seen from all the samples.

Table 3. Charge Transfer Studies between Alternating Terpolymers with F_4TCNQ

DD-terpolymers	F_4TCNQ	Cyano-ν(C≡N)[a]	charge transfer degree (δ)
ter-hexylthiophene-DD-stilbene	50 $_{mol\ \%}$	2197	0.92
ter-hexylthiophene-DD-biphenyl	50$_{mol\ \%}$	2211, 2195	0.49, 0.98
ter-hexylthiophene-DD-terphenyl	50$_{mol\ \%}$	2214, 2195	0.40, 0.98
ter-thiophene-DD-stilbene	50$_{mol\ \%}$	2214, 2196	0.40, 0.95
ter-bithiophene-DD-stilbene	50$_{mol\ \%}$	2196	0.95
ter-thienothiophene-DD-stilbene	50$_{mol\ \%}$	2212, 2194	0.46, 1
F_4TCNQ		2227	0

[a]Underlined peaks are considered the primary cyano vibrational band.

Results of FTIR of ter-hexylthiophene-DD-stilbene doped with F_4TCNQ from 5 to 100 mol % are shown in Figure 3. For all the samples, except ter-hexylthiophene-DD-stilbene doped with 50 and 100 mol % F_4TCNQ, shifts of

$$\delta = \frac{2\Delta\nu}{\nu_0}\left[1 - \frac{\nu_1^2}{\nu_0^2}\right]^{-1} \quad (1)$$

characteristic νC≡N bands from 2227 to 2194 cm^{-1} are observed in the FTIR from the strongest νC≡N bands of the anionic form of F_4TCNQ. For samples of ter-hexylthiophene-DD-stilbene doped with 50 and 100 mol % F_4TCNQ, shifts of characteristic νC≡N bands from 2227 to 2197 cm^{-1} are observed, which indicate partial charge transfer. The partial charge degree calculation using formula 1 gives a value of 0.92, which may simply be the error attributable to peak width. Therefore, all the samples show integer charge transfer on doping with F_4TCNQ.

The samples doped with >50 mol % show both integer charge transfer and partial charge transfer (δ = 0.49) on doping with excess F_4TCNQ with evidence of an absorption peak at 390 nm arising from the presence of excess neutral F_4TCNQ. These results are consistent with those of Neelamraju et al.'s work at high doping concentrations. In this work, organic conjugated semiconductors exhibit an increase in partial charge transfer states.[36] Albeit, the data were for solid state studies wherein it was surmised that crystalline segments gave unit charge transfer and amorphous regions were responsible for partial charge transfer. Given the very different nature of our DD terpolymers, such explanations may or may not be applicable for solution properties.

Absorption spectra for F_4TCNQ doped ter-hexylthiophene-DD-stilbene 5−100 mol % are shown in Figure 4. For samples of ter-hexylthiophene-DD-stilbene doped with more than 30 mol % F_4TCNQ, the absorption peaks at 755 and 855 nm of $F_4TCNQ^{\cdot-}$ corresponding with the D0 → D1 transition were seen. For samples of ter-hexylthiophene-DD-stilbene doped with >50 mol % F_4TCNQ, absorption peaks for $F_4TCNQ^{\cdot-}$ reach saturation. The peak at 390 nm shows excess neutral F_4TCNQ. All the peaks were normalized at a wavelength of 344 nm, which is the absorption peak of ter-hexylthiophene-DD-stilbene.

Modeling Studies. As in our previous work on DD and LL copolymers, we sought help in modeling the electronic behavior of these new systems. Two DFT approaches were used: VASP and Gaussian 16 (see the Experimental Section). In the former models, it is possible to discern cage-centered LUMOs for the model terpolymer components that are ≈6 eV above the HOMO for all examples modeled. However, these same calculations show band gaps of roughly 4 eV localized only on the aromatic components, suggesting no obvious conjugation via siloxane bonds, and VASP derived molecular

https://doi.org/10.1021/acs.macromol.2c01355
Macromolecules 2022, 55, 8106−8116

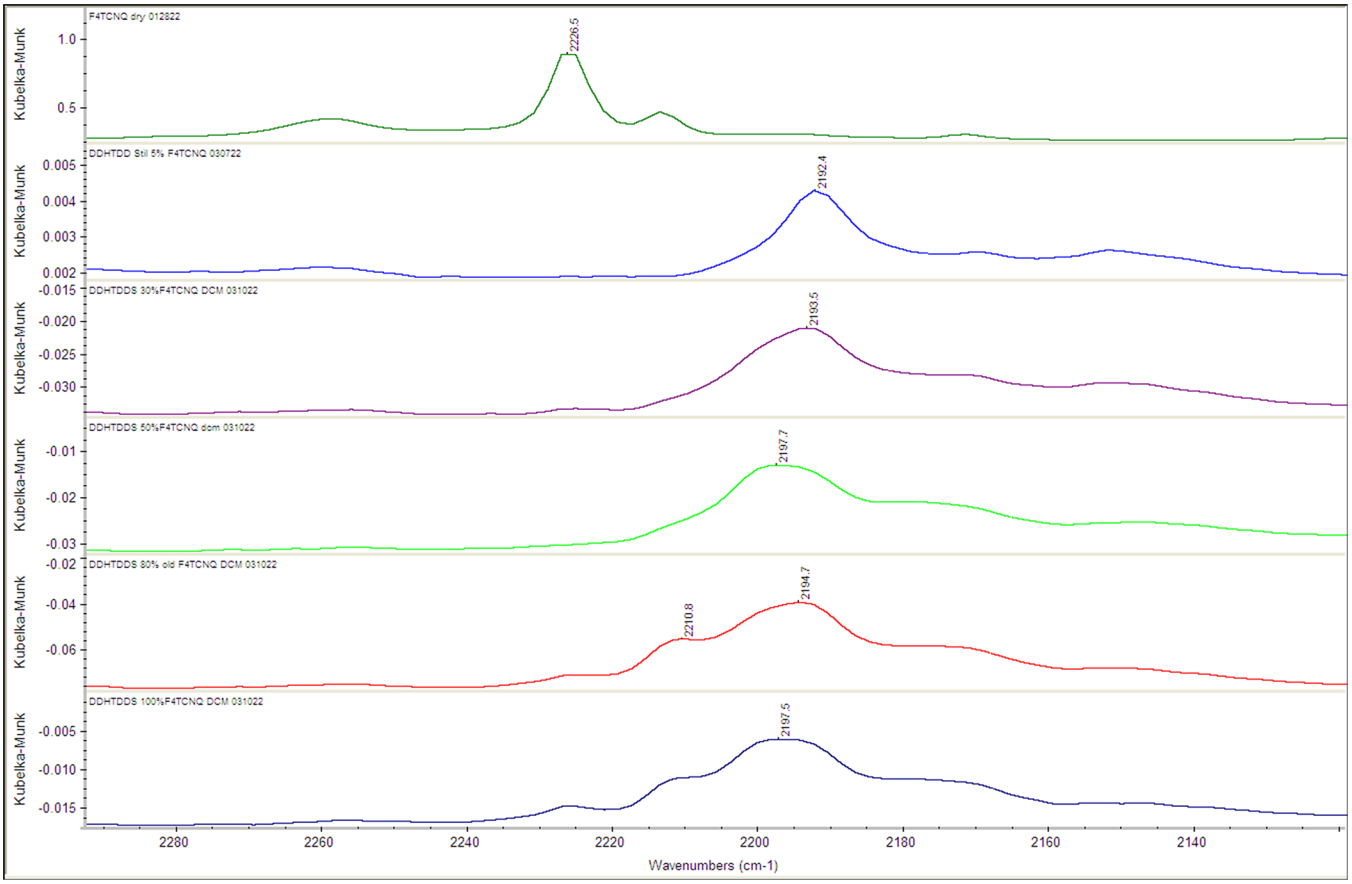

Figure 3. FTIR of ter-hexylthiophene-DD-stilbene doped with F_4TCNQ from 5 to 100 mol %.

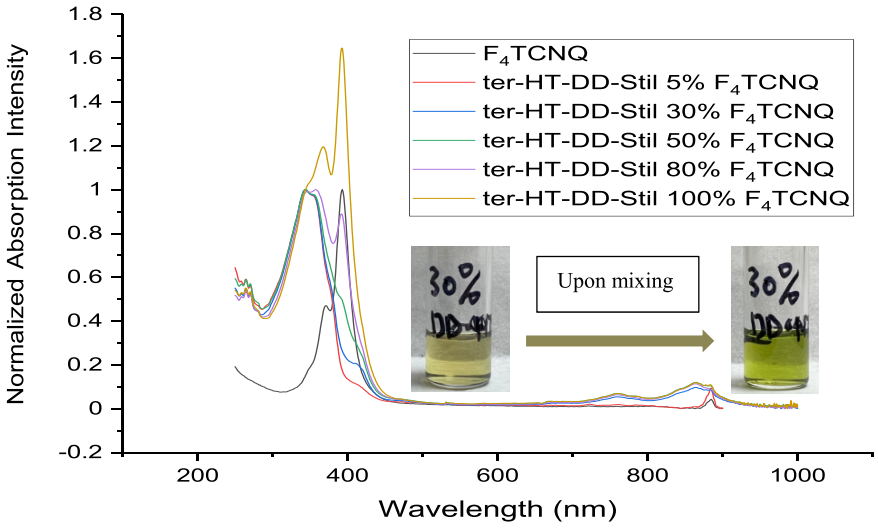

Figure 4. Absorption spectra for F_4TCNQ doped ter-hexylthiophene-DD-stilbene 5−100 mol %.

orbitals for ter-bithio-DD-stil are shown in Figure 5. More examples are found in Figures S74−S81.

For the Gaussian 16 modeling studies presented in Figure 6 and Figures S82−S89 and Table S8, we see HOMO-LUMO gaps of 5.5−6.5 eV. These studies also present calculated absorption/emission peaks that correspond directly to traditional π to π^* transitions. This approach also seems unable to predict the observed red-shifts seen, which would require LUMOs delocalized over several units.

One interpretation of these results is that there are nontraditional LUMOs participating in the photophysics of these terpolymers (and previous copolymers) that are, as of yet, not easily modeled using current methods and pointing to new opportunities for the modeling world.

Indeed, in efforts to be published in the near future,[37] we find that SQ and in particular DD copolymer and terpolymer photophysics behavior do not follow traditional expectations. We find that the fluorescence emission spectra of many if not all SQ-based systems studied so far defy Kasha's rule.[22] The

https://doi.org/10.1021/acs.macromol.2c01355
Macromolecules 2022, 55, 8106−8116

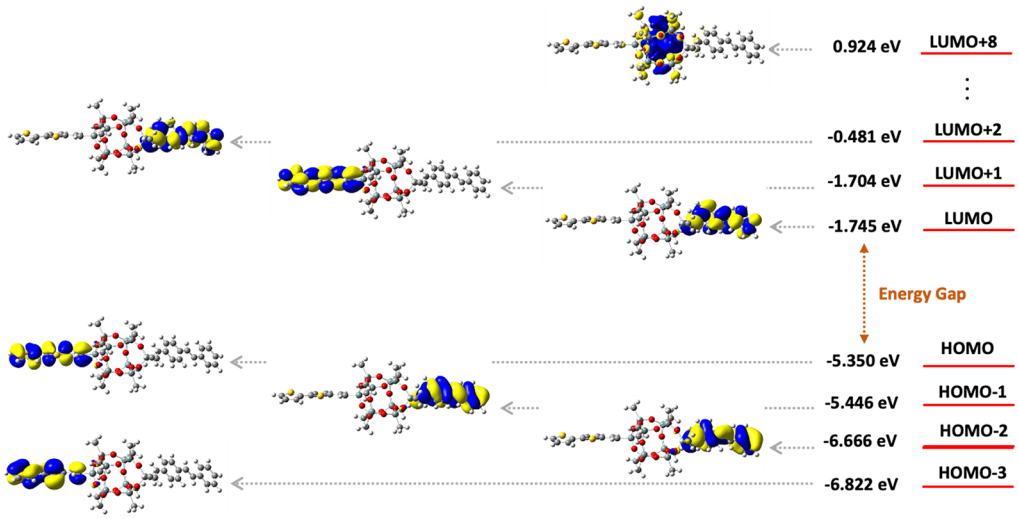

Figure 5. Example of VASP derived molecular orbitals for ter-bithio-DD-stil.

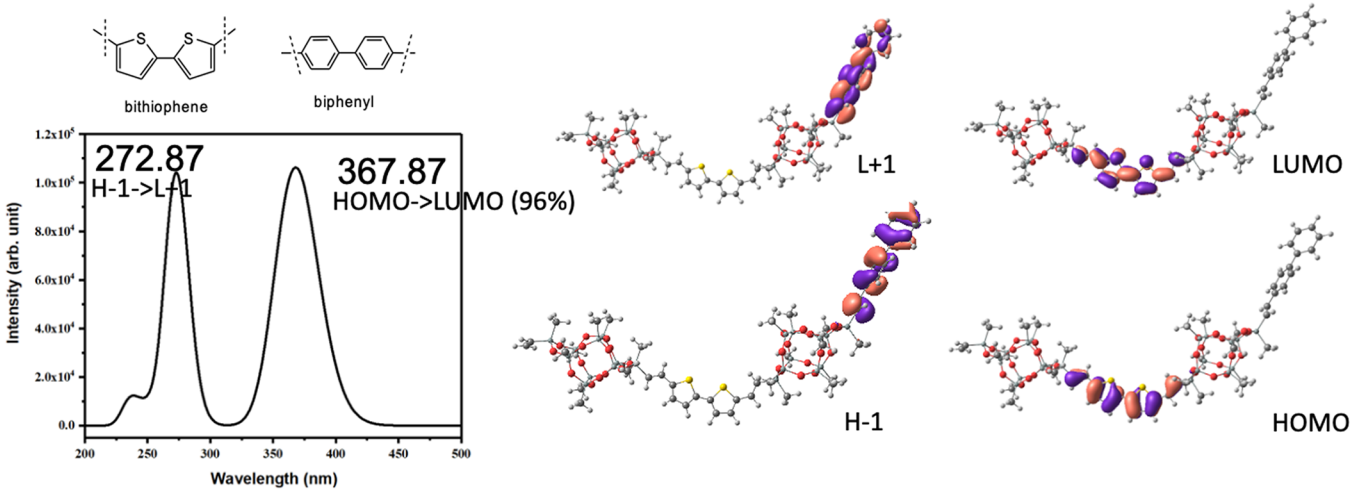

Figure 6. Example of Gaussian 16 derived molecular orbitals for DD-bithio-stil.

rule basically states that emission spectra will be primarily from the lowest excited state no matter what excitation wavelength is used. However, for most all SQ systems studied to date, there appears to be a notable shift of emission spectra depending on the excitation wavelength. As an immediate consequence, measurements of two photon absorption (2PA) cross sections and 2PA spectra that rely on detection of fluorescence, in particular, as reported recently,[22] may yield largely varying values, depending on what part of the fluorescence signal is being detected.

Carbon nanodots are also reported to exhibit excitation-dependent emissions contrary to Kasha's rule;[36,38] however, these results may be a consequence of the presence of impurities.[39,40] In the current efforts, the purities of the compounds studied here and previously are demonstrated via the various analytical tools employed.

CONCLUSIONS

This report details the synthesis and characterization of sets of conjugated terpolymers/oligomers derived from double decker silsesquioxanes. Two different synthetic routes were explored: the direct polymerization of DD with a 2:1:1 molar ratio of biphenyl and thiophene and polymerization step by step. Due to the different reaction rates between thiophene and biphenyl, polymerization step by step is a better method to yield alternating terpolymers. TGA indicates high thermal stabilities in air inherent with DD SQ cages. Photophysical studies of DD alternating terpolymers suggest that the absorption spectra display spectral characteristics from respective DD copolymers, while the emission spectra are an average of both copolymers. Electron transfer studies with F_4TNQ show both full and partial electron transfer possibly arising from two types of molecular association. This latter behavior may be tied to the presence of two emitting states that are excitation wavelength-dependent.[37]

These results indicate no ground-state electronic communication along the chain but provide additional strong evidence for unconventional conjugation in the excite state involving two different organic tethers extending along the length of the polymer despite the presence of disiloxane-capped links. Moreover, by incorporating terphenyl/stilbene to form terpolymers with DD and thiophene, the quantum yields are increased modestly with respect to the copolymer of DD and thiophene, pointing to potential opportunities to tailor the photophysical properties that are important in applications such as display panels.

https://doi.org/10.1021/acs.macromol.2c01355
Macromolecules 2022, 55, 8106−8116

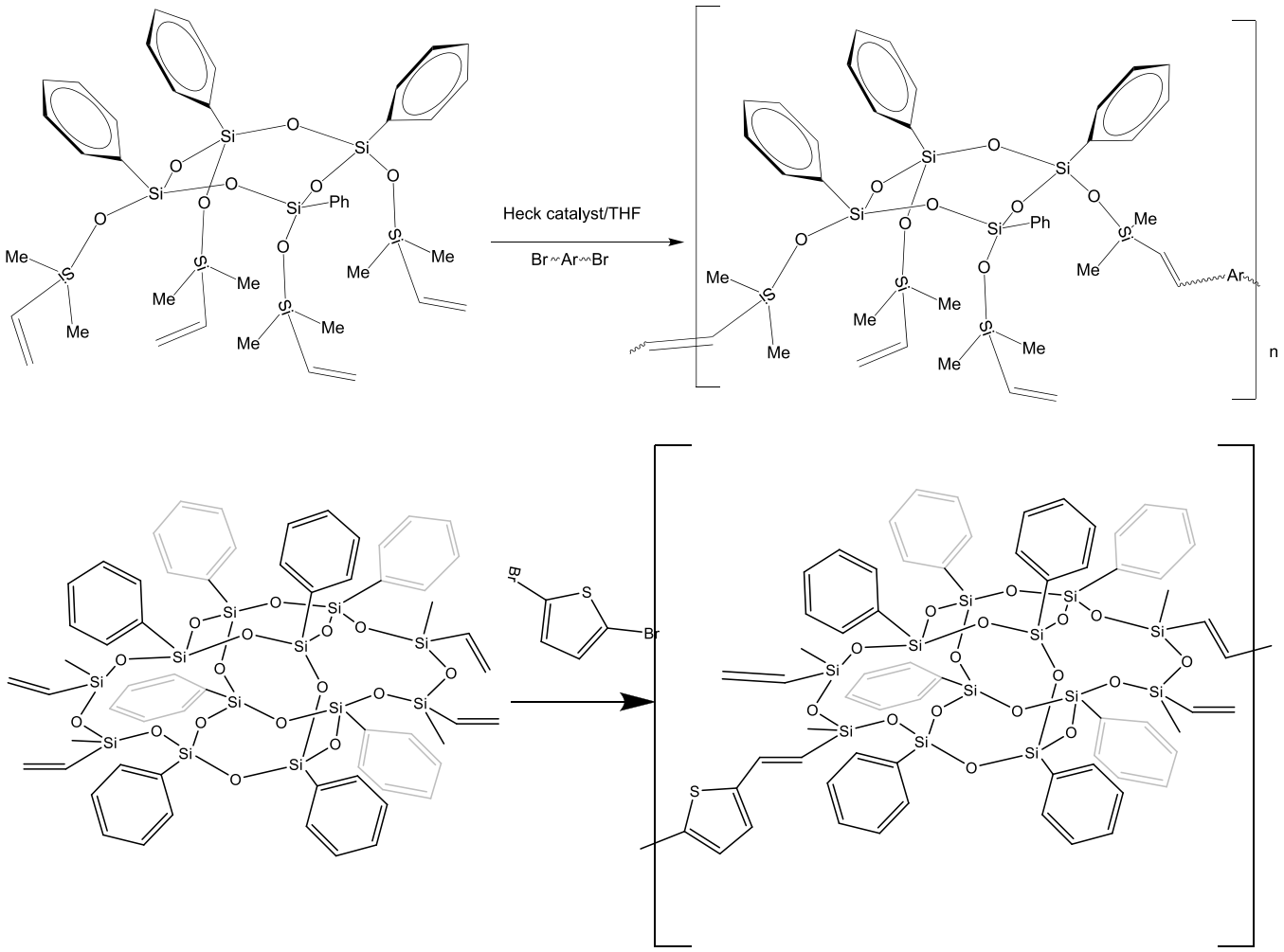

Figure 7. Heck catalyzed copolymerization of dibromoaryl monomers with the half cage tetra(methylvinylsiloxy)phenylsilsesquioxane and bis(methylvinylsiloxy)$_2$[PhSiO$_{1.5}$]$_8$.[41]

In a future paper, we will demonstrate further extensions of conjugation in siloxane-based copolymers, as illustrated in Figure 7.[41]

■ ASSOCIATED CONTENT

Supporting Information

The Supporting Information is available free of charge at https://pubs.acs.org/doi/10.1021/acs.macromol.2c01355.

MALDI, ^{1}H NMR spectra, ^{13}C NMR spectra, FTIR, light absorption and emission spectra, and modeling of molecular orbitals and UV−vis results for all compounds (PDF)

■ AUTHOR INFORMATION

Corresponding Author

Richard M. Laine − *Department of Materials Science and Engineering and Department of Macromolecular Science and Engineering, University of Michigan, Ann Arbor, Michigan 48105, United States;* orcid.org/0000-0003-4939-3514; Email: talsdad@umich.edu

Authors

Zijing Zhang − *Department of Materials Science and Engineering, University of Michigan, Ann Arbor, Michigan 48105, United States*

Jun Guan − *Department of Materials Science and Engineering, University of Michigan, Ann Arbor, Michigan 48105, United States*

Ramin Ansari − *Department of Chemical Engineering, University of Michigan, Ann Arbor, Michigan 48105, United States*

John Kieffer − *Department of Materials Science and Engineering, University of Michigan, Ann Arbor, Michigan 48105, United States;* orcid.org/0000-0002-1569-2631

Nuttapon Yodsin − *National Nanotechnology Center (NANOTEC), National Science and Technology Development Agency (NSTDA), Pathum Thani 12120, Thailand;* orcid.org/0000-0002-7124-7815

Siriporn Jungsuttiwong − *Department of Chemistry, Faculty of Science, Ubon Ratchathani University, Ubon Ratchathani 34190, Thailand;* orcid.org/0000-0001-5943-6878

Complete contact information is available at: https://pubs.acs.org/10.1021/acs.macromol.2c01355

Notes

The authors declare no competing financial interest.

■ ACKNOWLEDGMENTS

We gratefully acknowledge support from NSF Chemistry award no. CHE 2103602.

REFERENCES

(1) Voronkov, M. G.; Lavrent'yev, V. I. Polyhedral Oligosilsesquioxanes and Their Homo Derivatives. In *Inorganic Ring Systems*; Boschke, F. L., Dewar, M. J. S., Dunitz, J. D., Hafner, K., Heilbronner, E., Itô, S., Lehn, J.-M., Niedenzu, K., Raymond, K. N., Rees, C. W., Schäfer, K., Vögtle, F., Wittig, G., Series Eds.; Topics in Current Chemistry; Springer Berlin Heidelberg: Berlin, Heidelberg, 1982; Vol. *102*, pp. 199−236.

(2) Baney, R. H.; Itoh, M.; Sakakibara, A.; Suzuki, T. Silsesquioxanes. *Chem. Rev.* **1995**, *95*, 1409−1430.

(3) Loy, D. A.; Shea, K. J. Bridged Polysilsesquioxanes. Highly Porous Hybrid Organic-Inorganic Materials. *Chem. Rev.* **1995**, *95*, 1431−1442.

(4) Provatas, A.; Matisons, J. G. Synthesis and Applications of Silsesquioxanes. *Trends Polym. Sci.* **1997**, *5*, 327−322.

(5) Lichtenhan, J. Silsesquioxane-Based Polymers. In *Polymeric materials encyclopedia*; CRC Press: N.Y, 1996; Vol. *10*, pp. 7768−7777.

(6) Li, G.; Wang, L.; Ni, H.; Pittman, C. U., Jr. Polyhedral Oligomeric Silsesquioxane (POSS) Polymers and Copolymers: A Review. *J. Inorg. Organomet. Polym.* **2001**, *11*, 123−154.

(7) Duchateau, R. Incompletely Condensed Silsesquioxanes: Versatile Tools in Developing Silica-Supported Olefin Polymerization Catalysts. *Chem. Rev.* **2002**, *102*, 3525−3542.

(8) Phillips, S. H.; Haddad, T. S.; Tomczak, S. J. Developments in Nanoscience: Polyhedral Oligomeric Silsesquioxane (POSS)-Polymers. *Curr. Opin. Solid State Mater. Sci.* **2004**, *8*, 21−29.

(9) Abe, Y.; Gunji, T. Oligo- and Polysiloxanes. *Prog. Polym. Sci.* **2004**, *29*, 149−182.

(10) Kannan, R. Y.; Salacinski, H. J.; Butler, P. E.; Seifalian, A. M. Polyhedral Oligomeric Silsesquioxane Nanocomposites: The Next Generation Material for Biomedical Applications. *Acc. Chem. Res.* **2005**, *38*, 879−884.

(11) Laine, R. M. Nanobuilding Blocks Based on the $[OSiO_{1.5}]_x$ (X= 6, 8, 10) Octasilsesquioxanes. *J. Mater. Chem.* **2005**, *15*, 3725.

(12) Lickiss, P. D.; Rataboul, F. Fully Condensed Polyhedral Oligosilsesquioxanes (POSS): From Synthesis to Application. In *Advances in Organometallic Chemistry*; Elsevier, 2008; Vol. *57*, pp. 1−116.

(13) Wu, J.; Mather, P. T. POSS Polymers: Physical Properties and Biomaterials Applications. *Polym. Rev.* **2009**, *49*, 25−63.

(14) Cordes, D. B.; Lickiss, P. D.; Rataboul, F. Recent Developments in the Chemistry of Cubic Polyhedral Oligosilsesquioxanes. *Chem. Rev.* **2010**, *110*, 2081−2173.

(15) Laine, R. M.; Roll, M. F. Polyhedral Phenylsilsesquioxanes. *Macromolecules* **2011**, *44*, 1073−1109.

(16) *Applications of Polyhedral Oligomeric Silsesquioxanes*; Hartmann-Thompson, C., Ed.; Advances in silicon science; Springer: Dordrecht, 2011.

(17) Du, Y.; Liu, H. Triazine-Functionalized Silsesquioxane-Based Hybrid Porous Polymers for Efficient Photocatalytic Degradation of Both Acidic and Basic Dyes under Visible Light. *ChemCatChem* **2021**, *13*, 5178−5190.

(18) Sulaiman, S.; Bhaskar, A.; Zhang, J.; Guda, R.; Goodson, T.; Laine, R. M. Molecules with Perfect Cubic Symmetry as Nanobuilding Blocks for 3-D Assemblies. Elaboration of Octavinylsilsesquioxane. Unusual Luminescence Shifts May Indicate Extended Conjugation Involving the Silsesquioxane Core. *Chem. Mater.* **2008**, *20*, 5563−5573.

(19) Asuncion, M. Z.; Laine, R. M. Fluoride Rearrangement Reactions of Polyphenyl- and Polyvinylsilsesquioxanes as a Facile Route to Mixed Functional Phenyl, Vinyl T_{10} and T_{12} Silsesquioxanes. *J. Am. Chem. Soc.* **2010**, *132*, 3723−3736.

(20) Furgal, J. C.; Jung, J. H.; Goodson, T.; Laine, R. M. Analyzing Structure−Photophysical Property Relationships for Isolated T_8, T_{10}, and T_{12} Stilbenevinylsilsesquioxanes. *J. Am. Chem. Soc.* **2013**, *135*, 12259−12269.

(21) Imoto, H.; Ueda, Y.; Sato, Y.; Nakamura, M.; Mitamura, K.; Watase, S.; Naka, K. Corner- and Side-Opened Cage Silsesquioxanes: Structural Effects on the Materials Properties: Corner- and Side-Opened Cage Silsesquioxanes: Structural Effects on the Materials Properties. *Eur. J. Inorg. Chem.* **2020**, *2020*, 737−742.

(22) Guan, J.; Arias, J. J. R.; Tomobe, K.; Ansari, R.; de Marques, M. F. V.; Rebane, A.; Mahbub, S.; Furgal, J. C.; Yodsin, N.; Jungsuttiwong, S.; Hashemi, D.; Kieffer, J.; Laine, R. M. Unconventional Conjugation via $VinylMeSi(O-)_2$ Siloxane Bridges May Imbue Semiconducting Properties in $[Vinyl(Me)SiO(PhSiO_{1.5})_8$ OSi(Me)-Vinyl-Ar] Double-Decker Copolymers. *ACS Appl. Polym. Mater.* **2020**, 3894.

(23) Guan, J.; Sun, Z.; Ansari, R.; Liu, Y.; Endo, A.; Unno, M.; Ouali, A.; Mahbub, S.; Furgal, J. C.; Yodsin, N.; Jungsuttiwong, S.; Hashemi, D.; Kieffer, J.; Laine, R. M. Conjugated Copolymers That Shouldn't Be. *Angew. Chem., Int. Ed.* **2021**, *60*, 11115−11119.

(24) Guan, J.; Tomobe, K.; Madu, I.; Goodson, T.; Makhal, K.; Trinh, M. T.; Rand, S. C.; Yodsin, N.; Jungsuttiwong, S.; Laine, R. M. Photophysical Properties of Functionalized Double Decker Phenylsilsesquioxane Macromonomers: $[PhSiO_{1.5}]_8$ $[OSiMe_2]_2$ and $[PhSiO_{1.5}]_8$ $[O_{0.5}SiMe_3]_4$. Cage-Centered Lowest Unoccupied Molecular Orbitals Form Even When Two Cage Edge Bridges Are Removed, Verified by Modeling and Ultrafast Magnetic Light Scattering Experiments. *Macromolecules* **2019**, *52*, 7413−7422.

(25) Vosko, S. H.; Wilk, L.; Nusair, M. Accurate Spin-Dependent Electron Liquid Correlation Energies for Local Spin Density Calculations: A Critical Analysis. *Can. J. Phys.* **1980**, *58*, 1200−1211.

(26) Lee, C.; Yang, W.; Parr, R. G. Development of the Colle-Salvetti Correlation-Energy Formula into a Functional of the Electron Density. *Phys. Rev. B* **1988**, *37*, 785−789.

(27) Grimme, S.; Antony, J.; Ehrlich, S.; Krieg, H. A Consistent and Accurate *Ab Initio* Parametrization of Density Functional Dispersion Correction (DFT-D) for the 94 Elements H-Pu. *J. Chem. Phys.* **2010**, *132*, 154104.

(28) Grimme, S.; Ehrlich, S.; Goerigk, L. Effect of the Damping Function in Dispersion Corrected Density Functional Theory. *J. Comput. Chem.* **2011**, *32*, 1456−1465.

(29) Paier, J.; Hirschl, R.; Marsman, M.; Kresse, G. The Perdew−Burke−Ernzerhof Exchange-Correlation Functional Applied to the G2-1 Test Set Using a Plane-Wave Basis Set. *J. Chem. Phys.* **2005**, *122*, 234102.

(30) Perdew, J. P.; Burke, K.; Ernzerhof, M. Generalized Gradient Approximation Made Simple. *Phys. Rev. Lett.* **1996**, *77*, 3865−3868.

(31) Tkatchenko, A.; DiStasio, R. A.; Car, R.; Scheffler, M. Accurate and Efficient Method for Many-Body van Der Waals Interactions. *Phys. Rev. Lett.* **2012**, *108*, No. 236402.

(32) Ma, L.; Yuan, S.; Jiang, T.; Zhu, X.; Lu, C.; Li, X. Pd_4S/SiO_2: A Sulfur-Tolerant Palladium Catalyst for Catalytic Complete Oxidation of Methane. *Catalysts* **2019**, *9*, 410.

(33) Monai, M.; Montini, T.; Melchionna, M.; Duchoň, T.; Kúš, P.; Chen, C.; Tsud, N.; Nasi, L.; Prince, K. C.; Veltruská, K.; Matolín, V.; Khader, M. M.; Gorte, R. J.; Fornasiero, P. The Effect of Sulfur Dioxide on the Activity of Hierarchical Pd-Based Catalysts in Methane Combustion. *Appl. Catal., B* **2017**, *202*, 72−83.

(34) Tiancun, X.; Lidun, A.; Weimin, Z.; Shishan, S.; Guoxin, X. Mechanism of Sulfur Poisoning on Supported Noble Metal Catalyst ? The Adsorption and Transformation of Sulfur on Palladium Catalysts with Different Supports. *Catal. Lett.* **1992**, *12*, 287−296.

(35) Wilburn, M. S.; Epling, W. S. Sulfur Deactivation and Regeneration of Mono- and Bimetallic Pd-Pt Methane Oxidation Catalysts. *Appl. Catal., B* **2017**, *206*, 589−598.

(36) Neelamraju, B.; Watts, K. E.; Pemberton, J. E.; Ratcliff, E. L. Correlation of Coexistent Charge Transfer States in F_4 TCNQ-Doped P3HT with Microstructure. *J. Phys. Chem. Lett.* **2018**, *9*, 6871−6877.

(37) Rebane, A.; Guan, J.; Zhang, Z.; Richard, M. L. *Photophysics of Silsesquioxane Macromonomers, Copolymers and Terpolymers That Defy Kasha's Rule*, 2022.

(38) Righetto, M.; Carraro, F.; Privitera, A.; Marafon, G.; Moretto, A.; Ferrante, C. The Elusive Nature of Carbon Nanodot

https://doi.org/10.1021/acs.macromol.2c01355
Macromolecules 2022, 55, 8106−8116

Fluorescence: An Unconventional Perspective. *J. Phys. Chem. C* **2020**, *124*, 22314−22320.
(39) Soni, N.; Singh, S.; Sharma, S.; Batra, G.; Kaushik, K.; Rao, C.; Verma, N. C.; Mondal, B.; Yadav, A.; Nandi, C. K. Absorption and Emission of Light in Red Emissive Carbon Nanodots. *Chem. Sci.* **2021**, *12*, 3615−3626.
(40) Singhal, P.; Vats, B. G.; Pulhani, V. Origin of Solvent and Excitation Dependent Emission in Newly Synthesized Amphiphilic Carbon Dots. *J. Lumin.* **2022**, *244*, No. 118742.
(41) Rubio, J. J. A.; Unno, M.; Ouali, A.; Liu, Y.; Jungsuttiwong, S.; Kieffer, J.; Laine, R. M. More Extreme Examples of Extended Conjugation via Siloxane/Silsesquioxane Units.

https://doi.org/10.1021/acs.macromol.2c01355
Macromolecules 2022, 55, 8106−8116